Search for Physics beyond Standard Model at the Precision Frontiers

A. Aleksejevs and S. Wu
Grenfell campus of Memorial University, Corner Brook, Canada

S. Barkanova
Acadia University, Wolfville, Canada

Y. Bystritskiy
Joint Institute for Nuclear Research, Dubna, Russia

V. Zykunov
Belarussian State University of Transport, Gomel, Belarus

arXiv:1603.03006v1 [hep-ph] 7 Mar 2016

The article outlines the recent developments in the theoretical and computational approaches to the higher-order electroweak effects needed for the accurate interpretation of MOLLER and Belle II experimental data, and shows how new-physics particles enter at the one-loop level. By analyzing the effects of Z'-boson on the polarization asymmetry, we show how this hypothetical interaction carrier may influence the future experimental results.

I. INTRODUCTION

The recent availability of computer-algebra tools in particle physics research provides an unique opportunity to perform the Next-to-Leading-Order (NLO) and Next-to-NLO (NNLO) Standard Model (SM) calculations with the high degree of precision required by MOLLER and Belle II. Here, full SM calculations are required, with no approximations at the NLO level, and include leading order NNLO contributions, which can only be achieved with some degree of automatization. We do this for both MOLLER ($e^- + e^- \to e^- + e^-$) and Belle II ($e^+ + e^- \to \mu^+ + \mu^-$), and compare the results of calculations performed with the different sets of renormalization conditions using the on-shell renormalization. That provides a straightforward test of gauge invariance for the polarization asymmetry. A discrepancy between SM predictions and experimental measurements would signal the physics beyond the SM. Since MOLLER and Belle II are the most sensitive to the parity-violating (PV) interaction, we include U(1)$'$ extension of SM with a mass mixing scenario, which results in extension of SM by the parity-violating Z'-boson. Our analysis for Z' extends to NLO level giving us a refined set of constrains on the coupling and mass. First, we start with details on NLO and NNLO (quadratic) calculations for MOLLER and then continue with Belle II. In the second part of the paper, we provide results and analysis of the polarization asymmetry with Z'-boson present at LO and NLO orders.

II. SM PREDICTIONS FOR POLARIZATION ASYMMETRY IN MOLLER AND BELLE II

We consider two processes, $e^-_{k_1} + e^-_{k_2} \to e^-_{k_3} + e^-_{k_4}$, for MOLLER, and $e^+_{k_1} + e^-_{k_2} \to \mu^+_{k_3} + \mu^-_{k_4}$, for Belle II. For MOLLER, the most sensitive observable to PV new physics (aka Z') is the polarization asymmetry:

$$A_{LR} \;=\; \frac{\sigma_L - \sigma_R}{\sigma_L + \sigma_R} \simeq \frac{2\Re(M_\gamma M_Z^+ + M_\gamma M_{Z'}^+ + M_Z M_{Z'}^+)_{LR}}{\sigma_L + \sigma_R}. \tag{1}$$

In Eq.1, Z' will enter numerator of asymmetry through the interference term. For the $e^- + e^- \to e^- + e^-$ process, the asymmetry at LO order given by the following expression:

$$A^0_{LR(\mathrm{MOLLER})} \;=\; \frac{s}{m_W^2}\frac{y(1-y)}{1+y^4+(1-y)^4}\frac{1-4s_W^2}{s_W^2}. \tag{2}$$

Here, $y = -t/s$, the set of Mandelstam variables is used: $s = (k_1+k_2)^2$, $t = (k_3-k_1)^2$ and $u = (k_1-k_4)^2$, and the sine of Weinberg mixing angle is denoted as $s_W \equiv \sin\theta_W$. As one can see, the LO asymmetry is proportional to $1-4s_W^2$, which results in strong sensitivity to s_W^2. This provides an excellent opportunity for the precision measurements of s_W^2, or, accordingly, the measurement of the weak charge of electron. Although PV asymmetry in Eq.2 is quite small, the accuracy of modern experiments exceed the accuracy of the theoretical result at LO order; the NLO order calculations have been completed by number of authors [1–3]. Generally, we can express perturbative expansion (up

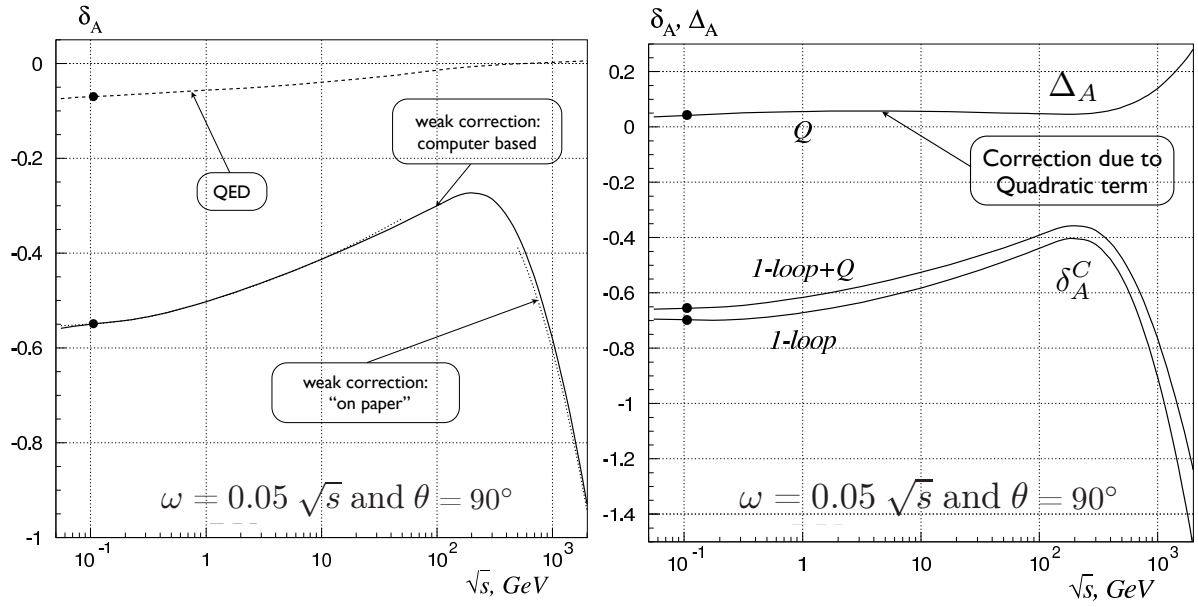

Figure 1: The graphs show corrections to the polarization asymmetry at the $\theta = 90^\circ$ and soft photon cut $\omega = 0.05\sqrt{s}$. In the left graph, dashed line shows correction due to QED effects, solid line represents weak correction based on semi-automated calculations and dotted line gives "on-paper" approximated calculations for the same correction. Right graph shows correction for pure quadratic ("Q") contribution (Δ_A), NLO ("1-loop") and NLO+NNLO ("1-loop-Q") results. Black dot on both graphs corresponds to the $E_{\rm lab} = 11$ GeV.

to NNLO) for differential scattering cross-section in orders of α as:

$$\frac{d\sigma}{d\cos\theta} = \frac{\pi^3}{2s}\Big|M_0 + M_1 + M_2\Big|^2 \simeq$$
$$\frac{\pi^3}{2s}\left(\alpha^2 M_0^{'} M_0^{'+} + \alpha^3 2\Re M_0^{'} M_1^{'+} + \alpha^4 (M_1^{'} M_1^{'+} + 2\Re M_0^{'} M_2^{'+})\right), \quad (3)$$

where matrix elements M_i are related to $M_i^{'}$ by $M_i = \alpha^{i+1} M_i^{'}$. The first term corresponds to LO, the second to NLO and the third forms NNLO contribution, which comprises from quadratic term ($\alpha^4 M_1^{'} M_1^{'+}$) and two-loops ($\alpha^4 2\Re M_0^{'} M_2^{'+}$) contribution. The NLO contribution to LO asymmetry is rather big ($\sim 69\%$) [3], and in order to match 1% MOLLER uncertainty, we calculated a full set NNLO (quadratic) [4] and leading order NNLO (two-loops) contributions [5] (and references therein). The precision is essential, so we control it in two ways. First, we applied "on paper" on-shell calculations using renormalization conditions of [10] and low energy approximations $\frac{r}{m^2_{Z,W}} \ll 1$ (here $r = s, |t|, |u|$). Second, we performed semi-automated [11–15] calculations for the full set of Feynman diagrams without any approximations and using renormalization conditions of [16]. This approach was implemented for NLO and NNLO (quadratic) contributions. The semi-automated full two-loop calculations are yet to be completed which is our next goal. Let us demonstrate how these two approaches compare to each other. First, we introduce a correction to the asymmetry, as:

$$\delta_A^C = \frac{A_{LR}^C - A_{LR}^0}{A_{LR}^0}, \quad (4)$$

where A_{LR}^C stands for the NLO-corrected asymmetry.

If we take $\alpha = 1/137.0359$, $m_W = 80.398$ GeV, $m_Z = 91.1876$ GeV and kinematics relevant to MOLLER experiment ($E_{\rm lab} = 11$ GeV), we can see in Fig.1 (right plot) that results obtained in both approaches differ less than 0.1%. We find that the NNLO (quadratic) contribution, Fig.1 (left plot),

$$\Delta_A = \frac{A_{LR}^{1-{\rm loop-Q}} - A_{LR}^{1-{\rm loop}}}{A_{LR}^0}, \quad (5)$$

$\theta,^\circ$	10	30	50	70	90	110	130	150	170
"on-paper"	0.0180	−0.0456	−0.0738	−0.0935	−0.1099	−0.1264	−0.1460	−0.1743	−0.2378
SA	0.0179	−0.0455	−0.0738	−0.0934	−0.1099	−0.1263	−0.1459	−0.1742	−0.2372

Table I: Relative NLO correction to unpolarized cross section δ^C_{00} in $e^+ + e^- \to \mu^+ + \mu^-$ process for the various angles in CM reference frame. Both approaches used soft-photon approximation in the treatment of infrared divergencies. Soft photon cut is $\omega = 0.05\sqrt{s}$.

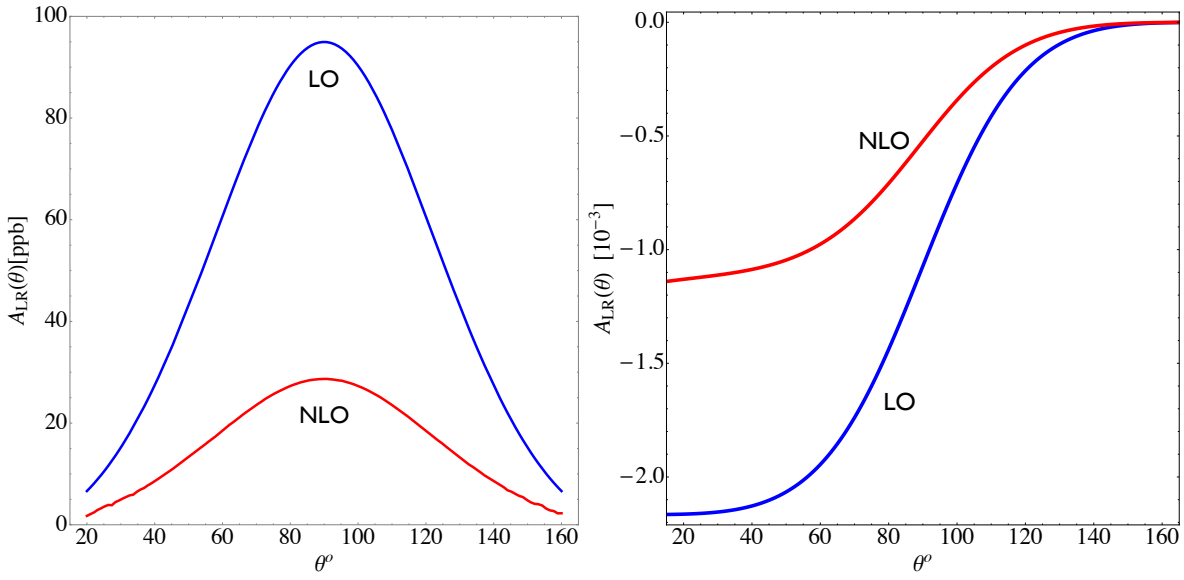

Figure 2: LO and NLO corrected polarization asymmetries for the MOLLER (left, $E_{\rm lab} = 11$ GeV) and Belle II (right, $\sqrt{s} = 10.57$ GeV) experiments for the $20^\circ < \theta < 160^\circ$ in the CM reference frame.

is responsible for $\sim 5\%$ suppression of the total correction at $E_{\rm lab} = 11$ GeV. This is a clear signal that, in the light of proposed precision experiments, the NNLO contributions are very important. Similar to the Moller process, $e^+ + e^- \to \mu^+ + \mu^-$ polarization asymmetry (first addressed in [17]), also shows strong sensitivity to the s^2_W:

$$A^0_{LR(\text{Belle II})} = -\frac{s}{4m^2_W}\frac{(y-1)^2}{2(y-1)y+1}\frac{1-4s^2_W}{s^2_W}. \tag{6}$$

We improve the precision by implementing the same two-way approach, for Belle II kinematics specifically, taking into account the full set of NLO electroweak corrections. For $\sqrt{s} = 10.57$ GeV, Table I shows our results for the NLO relative correction to unpolarized cross section ($\delta^C_{00} = \frac{\sigma^C_{00}-\sigma^0_{00}}{\sigma^0_{00}}$) computed using the semi-automated (SA) and "on-paper" calculation methods, in the on-shell renormalization. Evidently, difference in both approaches, for the broad range of scattering angles, is negligible. In Fig.2 we show the results for the NLO corrected asymmetries for both MOLLER and Belle II experiments.

Although the NLO contribution (Fig.2) for both processes is significant, judging by excellent agreement between two approaches presented here, the theoretical uncertainty at NLO level is at sub-percent level. However, that result does not include the NNLO contribution, needed to interpret ultra-precision measurements.

III. BEYOND THE STANDARD MODEL PHYSICS WITH DARK VECTOR

The discrepancy between experimental data and SM theoretical predictions would signal new interaction carriers. We use the simple U(1)′ extension of SM proposed in [18], which uses kinetic type of mixing between dark vector (A'_μ) and hyper-charge (B_μ) fields:

$$\mathfrak{L}_{kin} = -\frac{1}{4}B_{\mu\nu}B^{\mu\nu} + \frac{1}{2}\frac{\epsilon}{\cos\theta_W}B_{\mu\nu}A'^{\mu\nu} - \frac{1}{4}A'_{\mu\nu}A'^{\mu\nu}, \tag{7}$$

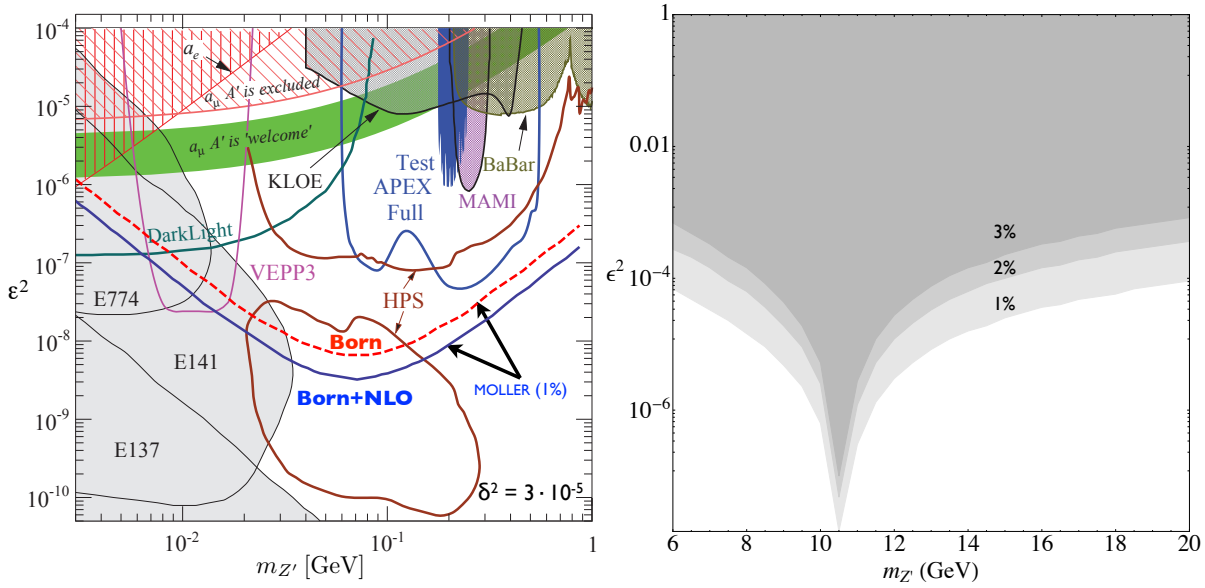

Figure 3: Exclusion plots for MOLLER (left) and Belle II (right). For MOLLER, we show exclusion for 1% deviation from SM prediction. Here, Z'_μ is included either at LO (Born) or up to NLO (Born+NLO) orders. Plot for Belle II shows up-to-NLO exclusion regions for 1%, 2% and 3% deviations from SM prediction. For both plots, we take $\delta^2 = 3 \cdot 10^{-5}$.

where fields tensors are given by $\{A'_{\mu\nu}, B_{\mu\nu}\} = \partial_\mu\{A'_\nu, B_\nu\} - \partial_\nu\{A'_\mu, B_\mu\}$, with $B_\mu = \cos\theta_W A_\mu - \sin\theta_W Z_\mu$ and ϵ is the $(B_\mu - A'_\mu)$ kinetic mixing parameter. With SM Higgs doublet plus the Higgs singlet (used for breaking the U(1)$'$ symmetry and giving mass to A'_μ), a Lagrangian describing interaction between the SM fermions and the dark vector boson A'_μ is:

$$\mathfrak{L}_{int} = -eQ_f\bar{f}\gamma^\mu f \cdot (V_\mu + \epsilon A'_\mu) - \frac{e}{\sin\theta_W\cos\theta_W}\bar{f}(c_V^f\gamma^\mu + c_A^f\gamma^\mu\gamma_5)f \cdot (Z_\mu + \epsilon_{Z'}A'_\mu). \quad (8)$$

Here, Q_f is the charge of the fermion in units of e, and the c_V^f and c_A^f constants are usual SM vector and axial-vector coupling strengths, respectively. As we can see from Eq.8, the A'_μ couples to fermions through both parity-conserving and violating terms, which is similar to the weak Z_μ coupling. That type of the A'_μ in [19] is called the dark Z'_μ-boson and derived from an additional mass mixing term characterized by mixing parameter $\epsilon_{Z'} = \frac{m_{Z'}}{m_Z}\delta$. Here, $m_{Z'}$ is the the mass of the dark Z'_μ-boson and δ is an arbitrary model-dependent parameter. The fact what Z'_μ is represented as a superposition of mixings between dark vector with electromagnetic and Z-boson fields makes it possible to include Z'_μ at NLO level. We include Z'_μ at NLO in order to match NLO calculations for our SM predictions. Our results are shown in the form of exclusion plots in Fig.3 for MOLLER (left) and Belle II (right).

In Fig.3, we explore a scenario of the small mixing ϵ and small Z'_μ mass, for MOLLER specifically. We show up-to-1% deviation from the SM central prediction exclusion plots for Z'_μ, which is included at LO and NLO orders. Inclusion of the Z'_μ at NLO order systematically increase exclusion region for ϵ for all masses of Z'_μ by about 25%. While this increase is not substantial, it could become an important factor in the determination of Z'_μ mass and coupling if Z'_μ is discovered. According to [19, 20], if no Z'_μ is discovered, MOLLER will exclude the region where Z'_μ is used to explain $(g-2)_\mu$ anomaly. For Belle II (right plot of Fig.3), we concentrate on the resonance region at $\sqrt{s} = 10.57$ GeV, where sensitivity of Belle II to the Z'_μ (up to NLO order) is the highest and is complimentary to the MOLLER experiment. For the $e^+ + e^- \to \mu^+ + \mu^-$ process, we also study the dependence of the asymmetry on the kinetic mixing parameter ϵ^2 and $m_{Z'}$, which is shown in Fig.4 (top two plots). If we take mass of Z' ($m_{Z'} = 8$ GeV), close to the $\sqrt{s} = 10.57$ GeV, the sensitivity of the asymmetry is the highest for $10^{-8} < \epsilon^2 < 10^{-4}$. In case of the fixed value for kinetic mixing, $\epsilon^2 = 10^{-5}$, the sensitivity of the asymmetry to the variations of $m_{Z'}$ is very weak except for the narrow region of resonance around $\sqrt{s} = 10.57$ GeV. This is because the leading $m_{Z'}$ dependence in asymmetry is determined by the ratio between kinetic mixing term ϵ^2 and denominator of Z' propagator ($\{t,s\} - m^2_{Z'}$). In t-channel (MOLLER), at $-t \to 0$ GeV^2, the asymmetry is proportional to $\epsilon^2/m^2_{Z'}$, and for light Z'_μ-boson it has a rather high sensitivity to $m_{Z'}$. In s-channel (Belle II), we get $A_{LR} \propto \epsilon^2/(s - m^2_{Z'})$, and for the $m^2_{Z'}/s \ll 1$ (light

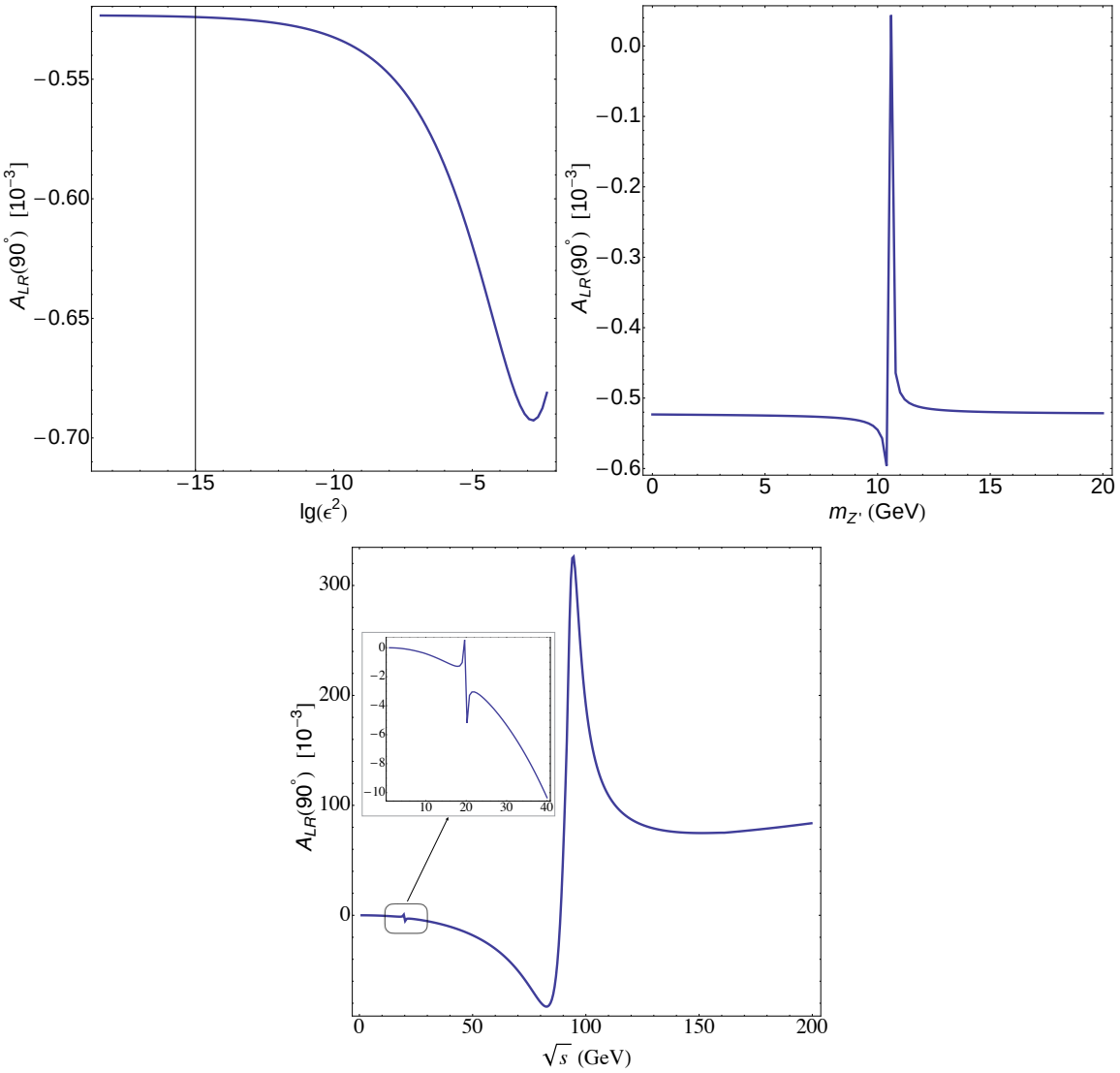

Figure 4: Figures show dependence of Belle II polarization asymmetry on mixing parameter ϵ^2 (top left, for $m_{Z'} = 8$ GeV), $m_{Z'}$ (top righ, for $\epsilon^2 = 10^{-5}$) and $\sqrt{s}$ (bottom center, for $m_{Z'} = 20$ GeV and $\epsilon^2 = 10^{-2}$). We choose for all graphs: $\delta^2 = 3 \cdot 10^{-5}$.

Z') the sensitivity is rather low. If we take $m^2_{Z'}/s \gg 1$ (heavy Z'), an overall contribution to the asymmetry due to Z' is suppressed so the effect of new physics becomes negligible. As a result, for Belle II, if mass of Z'_μ is around $\sqrt{s} = 10.57$ GeV, the sensitivity of that experiment to $m_{Z'}$ will be substantial. In Fig.4 (bottom, center), we show the overall dependence of asymmetry on the centre-of-mass energy. Here, we choose $m_{Z'} = 20$ GeV and $\epsilon^2 = 10^{-2}$, and it is evident that Z'-peak (if compared to Z-peak) is suppressed, which is due to the kinetic mixing parameter ϵ^2. The Z'-peak is relatively small, but, with the precision proposed by Belle II, it should be clearly detectable.

We conclude that the inclusion of NLO and NNLO electroweak radiative corrections is essential for the search of new physics at the precision frontier, and that the computer-algebra tools are indispensable for this task.

Acknowledgments

This work has been supported by the Natural Sciences and Engineering Research Council of Canada (NSERC).

References

[1] A. Czarnecki, W. J. Marciano, Phys. Rev. D53, 1066 (1996).
[2] A. Denner, S. Pozzorini, Eur. Phys. J. C7, 185 (1999).
[3] A. Aleksejevs, S. Barkanova, A. Ilyichev, V. Zykunov, Phys. Rev. D82, 093013 (2010).
[4] A. Aleksejevs, S. Barkanova, Y. Kolomensky, E. Kuraev, V. Zykunov, Phys. Rev. D85, 013007 (2012).
[5] A. Aleksejevs, S. Barkanova, Y. Bystritskiy, E. Kuraev, A. Ilyichev, V. Zykunov, arXiv:1202.0378 (2012).
[10] W. Hollik, Fortschr. Phys. 38, 165 (1990).
[11] T. Hahn, Comput. Phys. Commun., 140 418 (2001).
[12] T. Hahn, M. Perez-Victoria, Comput. Phys. Commun., 118, 153 (1999).
[13] J. Vermaseren, arXiv:math-ph/0010025 (2000).
[14] V. Shtabovenko, R. Mertig and F. Orellana, arXiv:1601.01167 (2016).
[15] R. Mertig, M. Böhm, and A. Denner, Comput. Phys. Commun., 64, 345-359 (1991).
[16] A. Denner, Fortsch. Phys. 41, 307 (1993).
[17] M. Bohm and W. Hollik, Nucl. Phys. B 204, 45 (1982).
[18] B. Holdom, Phys. Lett. B166, 196 (1986).
[19] H. Davoudiasl, H. Lee, W. Marciano, arXiv:1203.2947v2, Phys. Rev. D 85, 115019 (2012).
[20] A. Aleksejevs, S. Wu, S. Barkanova, V. Zykunov, arXiv:1410.6970 (2014).